

Separate As(V) from solution by mesoporous Y-Al binary oxide: batch experiments

Hang Liu, Caiyun Han, Liu Yang, Dekun Liu and Yongming Luo

ABSTRACT

Contaminant arsenic(V) has been regarded as one of the top-priority pollutants to remove from water. In this contribution, different mesoporous Y-Al binary oxides were prepared by the wet impregnation method via varying the molar ratio of Y/Al in the range of 0.029 to 0.116. The manufactured materials were employed as adsorbent to separate arsenic(V) from water. The adsorbent was characterized by N₂ adsorption-desorption isotherm, point of zero charge (PZC) and Fourier transform infrared (FT-IR). Furthermore, the effect of experimental parameters on adsorption performance was evaluated by batch experiments, including the molar ratio of Y/Al, adsorbent dosages and contact time, initial concentration, initial pH and temperature. The results indicated that the adsorbent presented an optimal adsorption performance for As(V) uptake when the molar ratio of Y/Al was 0.058. The obtained experimental data were best fitted by Langmuir isotherm and the maximum adsorption capacity was 60.93 mg/g at pH 6.6 ± 0.1. Additionally, according to the results of adsorption kinetics, it was pronounced that adsorption process was complied with pseudo-second-order model. The adsorption thermodynamic suggested that the adsorption of As(V) is endothermic and spontaneous natural. Moreover, based on the results of FT-IR, PZC and initial pH, it is demonstrated that ion-exchange and electrostatic interaction were the dominating adsorption mechanism.

Key words | adsorbent, adsorption capacity, arsenic(V), batch experiments, mechanism, mesoporous Y-Al binary oxide

Hang Liu
Caiyun Han (corresponding author)
Liu Yang
Dekun Liu
Yongming Luo
Faculty of Environmental Science and Engineering,
Kunming University of Science and Technology,
Kunming 650500,
China
E-mail: shenxifu@sina.com

INTRODUCTION

In recent decades, effective separation of As(V) species from solutions attracted much attention since this kind of species are the thermodynamically stable, are identified in overwhelming quantity and compose a seriously health threat (Matschullat 2000). Many kinds of techniques are designed to remove As(V), such as precipitation, ion-exchange, electro-coagulation, biological, adsorption, etc. (Vaclavikova *et al.* 2008). Among these available treatment approaches, adsorption has been regarded as the most effective method to remove As(V) due to the low cost, high efficiency, simple operation and less or no byproducts production (Han *et al.* 2013). Ordinarily, the most important factor in adsorption system is the adsorbent, which directly interacts with adsorbate. Therefore, the research relevant to efficient adsorbent quest has attracted extensive concern (Peng *et al.* 2016).

By far, most materials were employed as adsorbent to separate As(V) from solution, including activated carbon,

neutralized red mud (Genç *et al.* 2003) and ferrihydrite (Jain *et al.* 1999). The hydroxyl groups located on the adsorbent surface turn out to be the activated group to uptake As(V) (Li *et al.* 2010). Therefore, metal oxides have attracted much attention since they include abundant hydroxyl groups and offer high affinity to As(V) species. Specifically, Chen *et al.* (Chen *et al.* 2007) demonstrated that As(V) removal performance has significantly increased with graft iron oxide over activated carbon. Additionally, according to the report of Zhang *et al.* (Zhang *et al.* 2005), As(V) maximum adsorption capacity of Ce-Fe binary mixed oxide was 4 to 5 times higher compared to that of individual CeO₂ and Fe₃O₄. Furthermore, the metal (M)-OH group has been confirmed by Fourier transform infrared (FT-IR) and X-ray photoelectron spectroscopy (XPS) characterization techniques and it was the dominant bonding site of As(V). Therefore, it

was concluded that even more (M)-OH groups are capable of improving As(V) adsorption performance.

Recently, increasing porous material is developed with the discovery of M41S. Due to the excellent pore structure and high surface area, more active (M)-OH groups have been exposed over the surface of the adsorbent to contact the adsorbate. As an example, fast adsorption rate (equilibrium time less than 2 h) and high removal efficiency (94.7%) are exhibited in removal As(V) by mesoporous alumina, which proved to be superior compared to the commercial alumina which presents an equilibrium time of more than 9 h and a maximum removal efficiency below 50% (Han *et al.* 2013). Additionally, much attention has been focused on the composite metal oxides to increase the amount of active (M)-OH groups, while the eminent adsorption performance is observed in composite materials, such as Ce-Ti (Li *et al.* 2010) and Fe-Ti (Gupta & Ghosh 2009).

In this contribution, composite Y-Al binary oxide with mesoporous structure was synthesized by wet impregnation method under different molar ratio of Y/Al. The obtained materials were used as adsorbent to remove As(V) from water solution. The structure properties of the Y-Al binary oxide were characterized by N₂ adsorption-desorption isotherms, point of zero charge (PZC) and FT-IR. The adsorption performance was evaluated by performing batch experiments with variation of the operating parameters (initial pH, adsorption temperature, contact time and initial concentration). The experimental data were analyzed by Langmuir and Freundlich isotherms. Additionally, As(V) uptake mechanism was investigated in detail.

EXPERIMENTAL

Materials

Pluronic P123 (EO₂₀PO₇₀EO₂₀) was provided from Sigma-Aldrich. Aluminum tri-isopropoxide and Y(NO₃)₃·6H₂O were obtained from the Shanghai Chemical Regent Company of China. HCl and NaOH were supplied by Tianjin ShenTai Chemical Reagent Co., Ltd.

Prepared mesoporous Y-Al binary oxide

Wet impregnation method was adopted to prepare mesoporous Y-Al binary oxide. The carrier mesoporous alumina was initially synthesized under room temperature by the previous procedure (Han *et al.* 2013). Subsequently, the obtained mesoporous alumina was added into the aqueous solution of

Y(NO₃)₃·6H₂O under stirring. Finally, the well-mixed sample was dried at 100 °C for 12 h and then calcined at 400 °C for 3 h. The molar ratio of Y/Al in the mixture was 0.029, 0.058, 0.087 and 0.116, while the obtained solid samples were marked as Y-Al₁, Y-Al₂, Y-Al₃ and Y-Al₄, respectively.

Characterization

N₂ adsorption-desorption isotherms of Y-Al₁, Y-Al₂, Y-Al₃ and Y-Al₄ were determined by ASAP 2020 apparatus under -196 °C. The method of Barrett-Joyner-Halenda (BJH) and Brunauer-Emmett-Teller (BET) were adopted to calculate pore size distribution and specific surface area, respectively. The FT-IR spectroscopy was used to measure the surface group change by a Nicolet 560 IR spectrometer. The pH value for the point of zero charge (pH_{pzc}) was obtained by acid-base titration method.

Batch experiments

Batch experiments were conducted in a series of conical flasks by mixing As(V) solution and adsorbent mesoporous Y-Al binary oxide with magnetic stirring (200 rpm) at the scheduled time. The supernatant of the mixture, which was obtained by centrifuge, was used to measure the content of As(V). The As(V) concentration before and after adsorption process was measured by atomic fluorescence spectrometry (AFS-230E). The solution of HCl and NaOH was used to adjust the solution pH before adding adsorbent mesoporous Y-Al binary oxide. The removal efficiency and adsorption capacity were used to evaluate As(V) removal performance. The following Equations (1) and (2) were used to obtain the adsorption capacity and removal efficiency, respectively.

$$q_t = \frac{(C_0 - C_t) \times V}{m} \quad (1)$$

$$\eta = \frac{C_0 - C_t}{C_0} \times 100\% \quad (2)$$

Here, q_t (mg/g) is the adsorption capacity at time t . C_0 (mg/L) is the initial and concentration of As(V). C_t (mg/L) is the concentration of As(V) at time t . V (mL) is the volume of As(V) solution. m (g) is the dosage of adsorbent. η (%) is the removal efficiency at time t .

The adsorption isotherm experiments were carried out by different adsorbents (Y-Al₁, Y-Al₂, Y-Al₃ and Y-Al₄)

under ca. 20 °C and the contact time = 720 min. The adsorbent (0.1 g) was added into 50 mL solution (solid to liquid ratio = 2 g/L) of As(V) with various initial concentrations (4.47, 11.178, 44.703, 89.41 and 178.812 mg/L) at the fixing pH 6.6 ± 0.1 . Adsorption kinetics experiments were performed by varying solid to liquid ratio (0.4, 0.6, 1 and 1.4 g/L) under room temperature (ca. 20 °C) for a period of 720 min. And the other operating parameters were as follows: 50 mL solution with As(V) initial concentration of 44.703 mg/L, the pH was 6.6 ± 0.1 . The adsorption thermodynamic experiments were investigated by adding 0.05 g adsorbent (Y-Al₂) into 50 mL solution (solid to liquid ratio = 1 g/L) with As(V) initial concentration of 44.703 mg/L under different temperatures (20, 35, 50 and 65 °C) and the contact time = 720 min.

RESULTS AND DISCUSSION

Structure properties

The N₂ adsorption-desorption isotherms and pore size distributions of mesoporous Y-Al binary oxide including different molar ratios are illustrated in Figure 1. According to Figure 1, the isotherms shapes of the different Y-Al binary oxides are all found to be the type IV curve with H₁ hysteresis loop at (P/P₀) 0.35–0.90, based on the classification by International Union of Pure and Applied Chemistry (Sing 2009). A similar area (P/P₀) of hysteresis loop was observed in different mesoporous Y-Al binary oxides. This indicates that no significant distinction occurs in the pore size of Y-Al₁, Y-Al₂, Y-Al₃ and Y-Al₄, which is consistent with the results of pore size distribution (as presented in Figure 1) and the values of BJH pore diameter (as tabulated in Table S1, available with the online version of this paper). The BET surface area and BJH pore diameter of Y-Al₁, Y-Al₂, Y-Al₃ and Y-Al₄ are introduced in Table S1. It is pronounced that the BET surface area is decreased with the increasing Y/Al molar ratio.

To discern the surface group of mesoporous Y-Al binary oxide before and after uptake of As(V) under different initial pH, the FT-IR spectra are illustrated in Figure 2. It was concluded that three clear peaks at 3,628, 1,382 and 580 cm⁻¹ appeared in fresh Y-Al₂, which is respectively attributed to the vibration of basic hydroxyl group, Y-OH group and the overlap of M (metal)-O (Pavel *et al.* 2011). Nevertheless, the peaks at 3,628 and 1,382 cm⁻¹ were weakened and shifted to 1,210 and 1,156 cm⁻¹ after adsorption of As(V), which demonstrates that hydroxyl group on the surface of

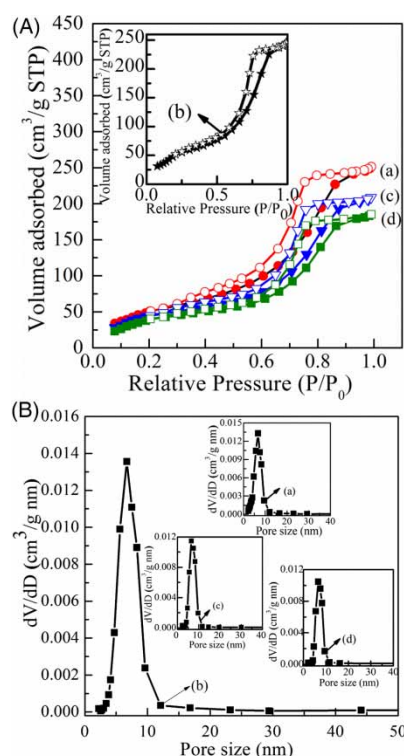


Figure 1 | (A) the N₂ adsorption-desorption isotherm and (B) the pore size distribution of (a) Y-Al₁, (b) Y-Al₂, (c) Y-Al₃ and (d) Y-Al₄.

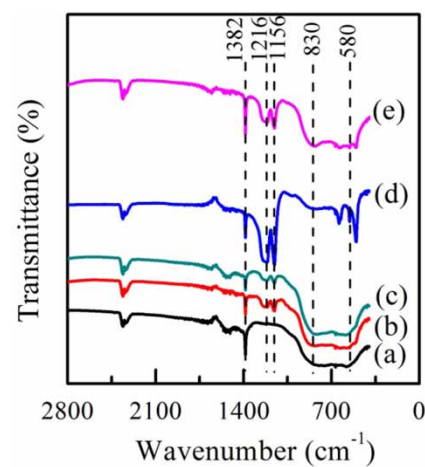


Figure 2 | The FT-IR of Y-Al₂ before and after adsorbed As(V) under different initial pH. (a) fresh Y-Al₂, (b) pH = 2.0, (c) pH = 6.6 ± 0.1, (d) pH = 4.0, (e) pH = 9.0.

mesoporous Y-Al binary oxide was reduced and involved in the adsorption process. Simultaneously, a new band appeared at ca. 830 cm⁻¹ after adsorption of As(V) (Curve b of Figure 1). It can be assigned to the vibration of As-O, which proves the removal of As(V) on the Y-Al₂ (Pillewan *et al.* 2011). Therefore, it indicated that ion exchange between

As(V) species and hydroxyl group was the adsorption mechanism.

As previously reported, the value of PZC was ca. 8.86, which is higher compared to that of pure alumina (8.3) due to the loading of (yttrium oxide) alkaline oxide (Tripathy & Raichur 2008). The result indicated that the surface of Y-Al₂ will be positive charges at pH < 8.86, which is in favour of binding As(V) anions. On the contrary, the deprotonation occurred on the surface of Y-Al₂ at pH > 8.86. Thus, the electrostatic repulsion (between negative charged surface of Y-Al₂ and As(V) anions) will be difficult to adsorption of As(V) anions.

As(V) separate performance

Effect of the molar ratio of Y/Al

According to previous research (He *et al.* 2015), the difference of adsorbent component would cause a significant variation in the adsorption performance. The effect of molar ratio of Y/Al on As(V) uptake is illustrated in Figure 3. It is found that As(V) adsorption capacity of mesoporous Y-Al binary oxide increased first when molar ratio of Y/Al increasing in the region of 0.029–0.058. It can be explained in that the available adsorption sites for As(V) uptake were increased with the loading of Y. And then As(V) uptake decreased with further increasing Y/Al molar ratio in the range of 0.058–0.116. This result might be associated with the monolayer distribution of yttrium oxide over the surface of alumina. The reduction of adsorption capacity at high molar ratio could be attributed to the aggregation and accumulate of the activated groups which will increase the

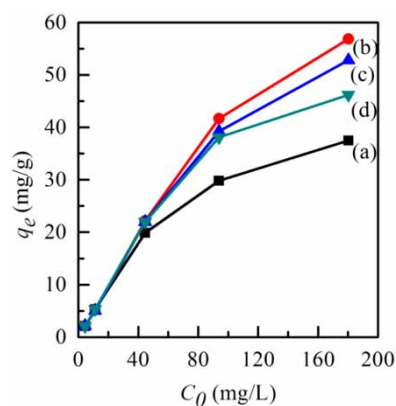


Figure 3 | As(V) uptake over (a) Y-Al₁, (b) Y-Al₂, (c) Y-Al₃ and (d) Y-Al₄. Experimental condition: adsorbent dosage = 0.1 g, volume = 50 mL, pH = 6.6 ± 0.1, adsorption temperature = 20 °C, As(V) concentration (C_0): 4.47, 11.178, 44.703, 89.41, 178.812 mg/L, respectively.

pore blockage (He *et al.* 2015). Therefore, the optimal adsorption capacity (56.86 mg/g) was obtained at Y-Al₂ (the molar ratio of Y/Al was 0.058), and Y-Al₂ was used in the following experimental procedure.

Effect of adsorbent dosages and contact time

The effect of adsorbent dosages and contact time on As(V) removal efficiency is illustrated in Figure 4. It is pronounced that the removal percentage was increased by increasing the amount of Y-Al₂, due to the development of adsorption sites at the fixed As(V) species. The maximum removal efficiency ca. 100% was obtained at adsorbent 0.1 g (the equilibrium time is ca. 150 min). This can be interpreted as a distribution of a variety of active sites in the adsorbent (Y-Al₂). Additionally, the time required to reach equilibrium is reduced by increasing the adsorbent dosages. As an example, the equilibrium time for 0.02 g and 0.05 g were 600 min and 300 min, respectively. This reveals that adsorption rate increases with the increase of active sites.

Effect of initial concentration

Initial concentration is a key parameter to assess the performance to removal contaminant from solution. The effect of initial As(V) concentration on removal percentage was investigated and the results are illustrated in Figure 5. It is pronounced that due to the increase of As(V) species in high concentration and the fixed dosage of Y-Al₂, As(V) removal percentage was decreased from 99.98% to 55.23% when an initial concentration increase from 4.47 mg/L to 89.41 mg/L, and the final As (V) concentration reached

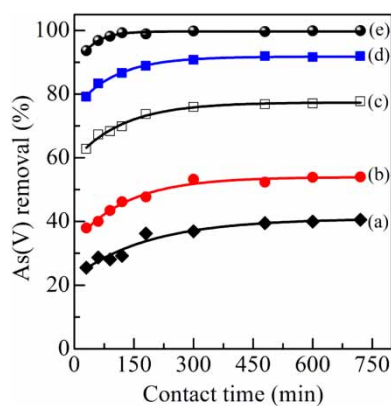


Figure 4 | Effect of adsorbent dosages and contact time on the removal of As(V) over Y-Al₂. (a) 0.02 g, (b) 0.03 g, (c) 0.05 g, (d) 0.07 g and (e) 0.1 g. Experimental condition: As(V) initial concentration = 44.703 mg/L, volume = 50 mL, pH = 6.6 ± 0.1, adsorption temperature = 20 °C.

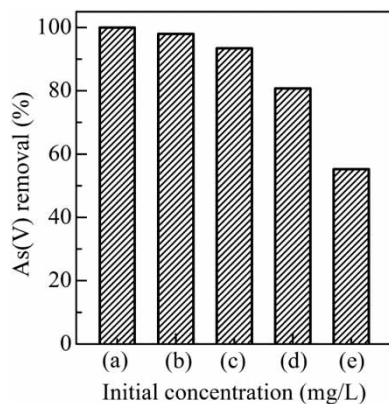


Figure 5 | Effect of initial concentration on the removal of As(V) over Y-Al₂. (a) 4.47, (b) 11.18, (c) 22.35, (d) 44.703 and (e) 89.41 mg/L. Experimental condition: adsorbent dosage = 0.05 g, volume = 50 mL, pH = 6.6 ± 0.1, adsorption temperature = 20 °C.

8.94 µg/L and 40.03 mg/L, respectively. World Health Organization stipulates the As(V) concentration must be lower than 10 µg/L (Martínez-Villafañe *et al.* 2009). This result indicates that Y-Al₂ is an efficient adsorbent for removing As(V) from low level of initial concentration (As(V) initial concentration lower than 4.47 mg/L) and achieved the 'drinking water' goal.

Effect of temperature

Temperature constitutes an important parameter in As(V) removal from wastewater. The effect of temperature on adsorption of As(V) was presented in Figure 6. The adsorption capacity increased from 36.08 to 39.42 mg/g with varying adsorption temperature from 20 to 65 °C. This

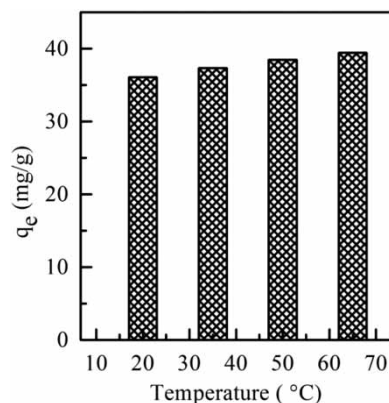


Figure 6 | Effect of temperature on the removal of As(V) over Y-Al₂. Experimental condition: As(V) initial concentration = 44.703 mg/L, adsorbent dosage = 0.05 g, volume = 50 mL, pH = 6.6 ± 0.1, adsorption temperature = 20, 35, 50 and 65 °C.

phenomenon can be attributed to the increase of collision frequency (between adsorbate and adsorbent) with the increase of adsorption temperature. It notes that increasing temperature contributed to the adsorption of As(V). And the detailed analyses were presented in adsorption thermodynamic study.

Effect of solution pH

Ordinary, pH is one of the most critical factors with significant influence on As(V) uptake, which will affect the form of arsenic and the surface potential of adsorbent. According to Figure 7, it can be found that the maximum removal efficiency was achieved at pH equal to 4. The removal efficiency increases by increasing of the pH from 2 to 4. And the reason can be attributed to the fact that the number of H₂AsO₄⁻ is increased in this pH region, which were sorbed over the protonated hydroxyl group of adsorbent Y-Al₂ via electrostatic interaction (Li *et al.* 2010). However, the removal efficiency sharply decreases when the initial pH further increases from 4 to 12. It can be ascribed to the concentration of OH⁻ which increases by pH further increase, thus resulting in the competition between arsenate and OH⁻ in the solution (Han *et al.* 2016b). In detail, when the initial pH varied from 4 to 8, the zeta potential of Y-Al₂ decreased which led to the weakness of electrostatic interaction. On the contrary, when the initial pH was equal to or higher than 9, the zeta potential of Y-Al₂ was negatively charged. Therefore, the removal efficiency decreases under alkaline conditions due to the repulsive force existing between the negatively charged surface and arsenate. Simultaneously, the main mechanism is ion-exchange between hydroxyl groups on the surface of Y-Al₂ and arsenate. These findings are in agreement with the result of FT-IR.

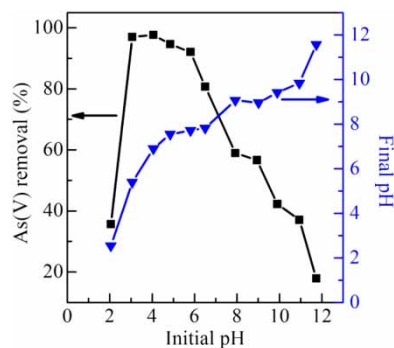


Figure 7 | Effect of initial pH on the removal of As(V) over Y-Al₂ and final pH. Experimental condition: As(V) initial concentration = 44.703 mg/L, adsorbent dosage = 0.05 g, volume = 50 mL, adsorption temperature = 20 °C.

By observing Figure 7, a very interesting phenomenon occurs. When the initial pH is lower than 8, the final pH becomes higher than the initial pH. Since the hydroxyl groups on surface of Y-Al₂ had been protonated (H⁺ in the solution were adsorbed), which results in the final pH increase. In contrast, when the initial pH is greater than 8, the final pH becomes lower compared to the initial pH. This occurs since the OH⁻ in the solution strongly compete with arsenate (HAsO₄²⁻ and AsO₄³⁻) for the active sites of Y-Al₂. In addition, according to previous research, it has been reported that alumina preferentially sorbed OH⁻ in the solution, which attributes to its weak acidity (Doukkali *et al.* 2012).

Adsorption isotherm

To investigate the adsorption characteristics of mesoporous Y-Al binary oxide for removing As(V), Langmuir and Freundlich isotherms were employed in this study. Linear Langmuir and Freundlich isotherms are represented by Equations (3) and (4), respectively.

$$\frac{C_e}{q_e} = \frac{1}{q_{\max}K_L} + \frac{C_e}{q_{\max}} \quad (3)$$

$$\ln q_e = \ln K_F + \frac{1}{n} \ln C_e \quad (4)$$

Here, K_L (L/mg) is the adsorption constant of Langmuir isotherm model, q_{\max} (mg/g) is the maximum adsorption capacity, C_e (mg/L) represents the concentration of As(V) at equilibrium, q_e (mg/g) is adsorption capacity at equilibrium, K_F and $1/n$ symbolize the Freundlich constant related to the adsorption capacity and adsorption intensity, respectively.

The adsorption isotherm of the adsorbent mesoporous Y-Al binary oxide was investigated at pH 6.6 ± 0.1 and the corresponding results are presented in Figure S2 (available with the online version of this paper). The experimental

data were evaluated by Langmuir and Freundlich isotherm equations and the corresponding parameters were summarized in Table 1. It was pronounced that the correlation coefficient (R^2) of Langmuir isotherm model was significantly higher compared to Freundlich isotherm model. It was indicated that the adsorption behavior corresponds efficiently to Langmuir isotherm model rather than Freundlich isotherm model, which also reveals that the As(V) uptake belongs to a monolayer adsorption (Deng & Yu 2012a). Meanwhile, the preferable fitting between experimental data and Langmuir isotherm model reveals the fact that the adsorption reactions occurred on the homogeneous surface of Y-Al binary oxide (Zhang *et al.* 2013).

As presented in Table 1, the maximum adsorption capacity is 60.93 mg/g. To evaluate the performance of the adsorbent Y-Al binary oxide for As(V) uptake, the comparison of adsorption capacity of other materials was also listed in Table 2. It is concluded that the adsorption capacity of the adsorbent Y-Al binary oxide is higher than previous reported materials, which indicates that the adsorbent Y-Al binary oxide represents one of the most promising adsorbents for separating As(V) from wastewater.

Adsorption kinetics

Adsorption kinetics of As(V) represents a key parameter for understanding the adsorption mechanism and investigating adsorption rate, which contributes to guide and design the adsorption experiment. Linear pseudo-first-order model (Equation (5)) and pseudo-second-order model (Equation (6)) were employed to evaluate the experimental data.

$$\ln(q_e - q_t) = \ln q_e - K_1 t \quad (5)$$

$$\frac{t}{q_t} = \frac{1}{K_2 q_e^2} + \frac{1}{q_e} t \quad (6)$$

On the above equations, t (min) is the contact time, q_t (mg/g) is the adsorption capacity at any time t , q_e (mg/g)

Table 1 | The parameters of Langmuir and Freundlich isotherm for the effect of the molar ratio of Y/Al on As(V) adsorption

Langmuir isotherm				Freundlich isotherm			
Y/Al	q_{\max} (mg/g)	K_L	R^2	Y/Al	K_F	$1/n$	R^2
0.029	39.00	0.1760	0.9951	0.029	5.6446	0.4673	0.8732
0.058	60.93	0.2053	0.9785	0.058	12.3414	0.5513	0.1497
0.087	57.14	0.1831	0.9798	0.087	9.1559	0.4717	0.5375
0.116	48.80	0.3019	0.9922	0.116	9.7141	0.4621	0.5158

Table 2 | Comparison of adsorption capacity of As(V) adsorbed over other materials

Adsorbent	Adsorption capacity (mg/g)	Source
Mesoporous alumina	36.6	Han et al. (2013)
Alumina	<20	Tchieda et al. (2016)
γ -Al ₂ O ₃	26.60	Chiavola et al. (2016)
Sigma- Al ₂ O ₃	8.64	Chiavola et al. (2016)
Al-Ti	9.50	Chiavola et al. (2016)
Mesoporous Y-Al binary oxide	60.93	This work

represents adsorption capacity at equilibrium, K_1 (min⁻¹) and K_2 (g/(mg·min)) are the adsorption rate constant of pseudo-first-order model and pseudo-second-order model, respectively.

The curves and parameters of the above two kinetics models are summarized in Figure 8 and Table S2 (available with the online version of this paper), respectively. It is pronounced that the correlation coefficients (R^2) of pseudo-first-order are lower than that of pseudo-second-order model. In addition, the q_e of calculation ($q_{e\text{ (cal)}}$) of pseudo-second-order model is remarkably higher than pseudo-first-order model, which is in agreement with the value of experiment ($q_{e\text{ (exp)}}$). Therefore, it can be considered that pseudo-second-order model is the appropriate to analyse the process of As(V) uptake over Y-Al with a variety of dosages (Swain et al. 2011). This result also reveals that the adsorption process was chemisorption and the adsorption reactions were the rate-limiting step mechanism (Deng & Yu 2012b).

Thermodynamic study

The feasibility and spontaneity of the adsorption process were determined by ΔG^0 , ΔH^0 and ΔS^0 . And the related parameters of thermodynamic were calculated by the following equations:

$$\Delta G^0 = -RT \ln K_a \quad (7)$$

$$K_a = \frac{\Delta S^0}{R} - \frac{\Delta H^0}{R} \times \frac{1}{T} \quad (8)$$

Here, ΔG^0 (KJ/mol) is the change in free energy. R (8.314 J/(mol·K)) is the ideal gas constant. T (K) is the

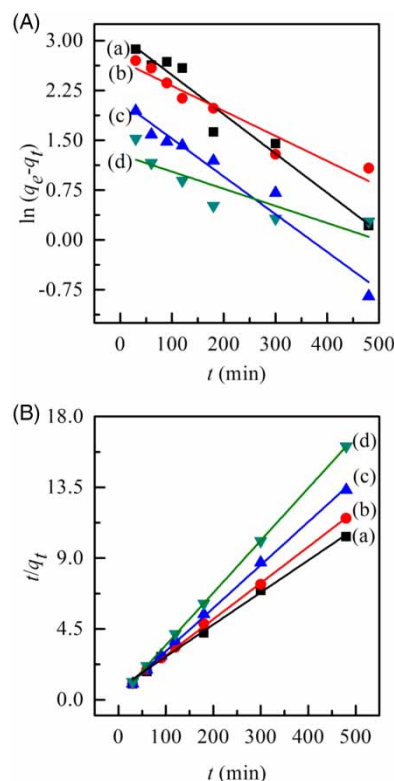


Figure 8 | (A) Pseudo-first-order and (B) pseudo-second-order curves of adsorption kinetics with arsenate adsorbed over Y-Al with different dosages (a) 0.02 g, (b) 0.03 g, (c) 0.05 g, (d) 0.07 g. Experimental condition: As(V) initial concentration = 44.703 mg/L, volume = 50 mL (solid to liquid ratio = 0.4, 0.6, 1 and 1.4 g/L, respectively), pH = 6.6 ± 0.1, adsorption temperature = 20 °C, contact time = 720 min.

absolute temperature. K_a (L/g) is the equilibrium constant which is calculated by q_e/C_e . ΔH^0 (KJ/mol) is the change in enthalpy. ΔS^0 (J/(mol·K)) is the change in entropy.

The value of ΔH^0 and ΔS^0 are determined by the slope and intercept of the linear plot of K_a vs. $1/T$ which was illustrated in Figure S3. And the value of all thermodynamic parameters were listed in Table S3. (Figure S3 and Table S3 are available with the online version of this paper.) As shown in Table S3, the positive value of ΔH^0 (10.59 KJ/mol) indicates that the adsorption reaction of As(V) is endothermic. Based on the positive value of ΔS^0 , it suggests that the randomness at the solid/liquid interface increased with the increasing of the adsorption temperature during the adsorption process. In addition, the negative value of ΔG^0 (-3.14, -4.15, -4.88 and -5.65 KJ/mol) reveals that the spontaneous nature of As(V) uptake on the surface of Y-Al₂. And the reduction of ΔG^0 with the further increasing of temperature deems that rising temperature can promote the adsorption capacity of As(V) and this result is according with the above result (Figure 6).

CONCLUSION

In this work, the mesoporous Y-Al binary oxide was successfully prepared by incipient wetness impregnation and used as the adsorbent for As(V) uptake. It was demonstrated that the adsorbent has an optimal adsorption performance for As(V) uptake when the molar ratio of Y/Al was 0.058. The adsorption performance of Y-Al followed the order of Y-Al₂ > Y-Al₃ > Y-Al₄ > Y-Al₁. According to the experimental results, the process of As(V) uptake was influenced by many parameters, including the molar ratio of Y/Al, adsorbent dosages and contact time, initial concentration, initial pH and adsorption temperature. Furthermore, the maximum adsorption capacity was 60.93 mg/g, which was calculated from Langmuir isotherm model. The study of kinetics depicted that the adsorption process corresponds to a pseudo-second-order model and chemisorption was the main interaction between adsorbate (As(V)) and adsorbent (Y-Al). The thermodynamic study pointed out that As(V) uptake over Y-Al₂ was spontaneous and endothermic. Finally, based on the results of FT-IR, pH_{pzc} and initial pH, it was pronounced that ion-exchange and electrostatic interaction were involved in the adsorption process at pH ≥ 9 and pH < 9, respectively.

ACKNOWLEDGEMENTS

We gratefully acknowledge the support of this work by Natural Science Foundation of China (Grant No. 21507051, 21767016 and U1402233), Personnel Training Funds of Kunming University of Science and Technology (KKS201422060), and Young Academic and Technical Leader Raising Foundation of Yunnan Province (Grant No. 2008py010).

REFERENCES

- Chen, W., Parette, R., Zou, J., Cannon, F. S. & Dempsey, B. A. 2007 Arsenic removal by iron-modified activated carbon. *Water Research* **41** (9), 1851–1858.
- Chiavola, A., Tchieda, V. K., D'Amato, E., Chianese, A. & Kanaev, A. 2016 Synthesis and characterization of nanometric titania coated on granular alumina for arsenic removal. *Chemical Engineering Transactions* **47**, 331–336.
- Deng, H. & Yu, X. 2012a Fluoride sorption by metal ion-loaded fibrous protein. *Industrial Engineering Chemistry Research* **51** (5), 2419–2427.
- Deng, H. & Yu, X. 2012b Adsorption of fluoride, arsenate and phosphate in aqueous solution by cerium impregnated fibrous protein. *Chemical Engineering Journal* **184** (3), 205–212.
- Doukkali, M. El., Iriondo, A., Arias, P. L., Cambra, J. F., Gandarias, I. & Barrio, V. L. 2012 Bioethanol/glycerol mixture steam reforming over Pt and PtNi supported on lanthana or ceria doped alumina catalysts. *International Journal of Hydrogen Energy* **37** (10), 8298–8309.
- Genç, H., Tjell, J. C., McConchie, D. & Schuiling, O. 2003 Adsorption of arsenate from water using neutralized red mud. *Journal of Colloid and Interface Science* **264** (2), 327–334.
- Gupta, K. & Ghosh, U. C. 2009 Arsenic removal using hydrous nanostructure iron(III)-titanium(IV) binary mixed oxide from aqueous solution. *Journal of Hazardous Materials* **161** (2–3), 884–892.
- Han, C. Y., Li, H. Y., Pu, H. P., Yu, H. L., Deng, L., Huang, S. & Luo, Y. M. 2013 Synthesis and characterization of mesoporous alumina and their performances for removing arsenic(V). *Chemical Engineering Journal* **217** (2), 1–9.
- Han, C. Y., Liu, H., Chen, H. R., Zhang, L. M., Wan, G. P., Shan, X., Deng, J. S. & Luo, Y. M. 2016a Adsorption performance and mechanism of As(V) uptake over mesoporous Y-Al binary oxide. *Journal of the Taiwan Institute of Chemical Engineers* **65**, 204–211.
- Han, C. Y., Zhang, L. M., Chen, H. R., Shan, X., Li, X. T., Zhu, W. J. & Luo, Y. M. 2016b Removal As (V) by sulfated mesoporous Fe-Al bimetallic adsorbent: adsorption performance and uptake mechanism. *Journal of Environmental Chemical Engineering* **4** (1), 711–718.
- He, S. F., Han, C. Y., Wang, H., Zhu, W. J., He, S. Y., He, D. D. & Luo, Y. M. 2015 Uptake of arsenic(V) using alumina functionalized highly ordered mesoporous SBA-15 (Alx-SBA-15) as an effective adsorbent. *Journal of Chemical and Engineering Data* **60** (5), 1300–1310.
- Jain, A., Raven, K. P. & Loeppert, R. H. 1999 Arsenite and arsenate adsorption on surface ferrihydrite: charge reduction and net OH-release stoichiometry. *Environmental Science & Technology* **33** (8), 1179–1184.
- Li, Z. J., Deng, S. B., Yu, G., Huang, J. & Lim, V. C. 2010 As(V) and As(III) removal from water by a Ce-Ti oxide adsorbent: behavior and mechanism. *Chemical Engineering Journal* **161** (1–2), 106–113.
- Martínez-Villafañe, J. F., Monteroocampo, C. & Garcíalara, A. M. 2009 Energy and electrode consumption analysis of electrocoagulation for the removal of arsenic from underground water. *Journal of Hazardous Materials* **172** (2), 1617–1622.
- Matschullat, J. 2000 Arsenic in the geosphere—a review. *Science of the Total Environment* **249** (1–3), 297–312.
- Pavel, O. D., Cojocaru, B., Angelescu, E. & Parvulescu, V. I. 2011 The activity of yttrium-modified Mg, Al hydrotalcites in the epoxidation of styrene with hydrogen peroxide. *Applied Catalysis A General* **403** (1–2), 83–90.

- Peng, B., Song, T. T., Wang, T., Chai, L. Y., Yang, W. C., Li, X. R., Li, C. F. & Wang, H. Y. 2016 Facile synthesis of $\text{Fe}_3\text{O}_4/\text{Cu}(\text{OH})_2$ composites and their arsenic adsorption application. *Chemical Engineering Journal* **299**, 15–22.
- Pillewan, P., Mukherjee, S., Roychowdhury, T., Das, S., Bansiwala, A. & Rayalu, S. 2011 Removal of As(III) and As(V) from water by copper oxide incorporated mesoporous alumina. *Journal of Hazardous Materials* **186** (1), 367–375.
- Sing, K. S. W. 2009 Reporting physisorption data for gas/solid systems with special reference to the determination of surface area and porosity (Recommendations 1984). *Pure & Applied Chemistry* **57** (11), 2201–2218.
- Swain, S. K., Patnaik, T., Singh, V. K., Jha, Usha, Patelet, R. K. & Dey, R. K. 2011 Kinetics, equilibrium and thermodynamic aspects of removal of fluoride from drinking water using meso-structured zirconium phosphate. *Chemical Engineering Journal* **171** (3), 1218–1226.
- Tchida, V. K., D'Amato, E., Chiavola, A., Parisi, M., Chianese, A., Amamra, M. & Kanaev, A. 2016 Removal of arsenic by alumina: effects of material size, additives and water contaminants. *CLEAN- Soil Air, Water* **44** (5), 496–505.
- Tripathy, S. S. & Raichur, A. M. 2008 Enhanced adsorption capacity of activated alumina by impregnation with alum for removal of As(V) from water. *Chemical Engineering Journal* **138** (1–3), 179–186.
- Vaclavikova, M., Gallios, G. P., Hredzak, S. & Jakabsky, S. 2008 Removal of arsenic from water streams: an overview of available techniques. *Clean Technologies and Environmental* **10** (1), 89–95.
- Zhang, Y., Yang, M., Dou, X. M., He, H. & Wang, D. S. 2005 Arsenate adsorption on an Fe-Ce bimetal oxide adsorbent: role of surface properties. *Environmental Science & Technology* **39** (18), 7246–7250.
- Zhang, G. S., Ren, Z. M., Zhang, X. W. & Chen, J. 2013 Nanostructured iron(III)-copper(II) binary oxide: a novel adsorbent for enhanced arsenic removal from aqueous solutions. *Water Research* **47** (12), 4022–4031.

First received 6 July 2017; accepted in revised form 15 November 2017. Available online 29 November 2017